

**Medical Nuclear Supply Chain Design:  
A Tractable Network Model and Computational Approach**

Anna Nagurney\*

Department of Finance and Operations Management

Isenberg School of Management

University of Massachusetts, Amherst, Massachusetts 01003; email: nagurney@isenberg.umass.edu

and

School of Business, Economics and Law

University of Gothenburg, Gothenburg, Sweden

Ladimer S. Nagurney

Department of Electrical and Computer Engineering

University of Hartford, West Hartford, Connecticut 06117; email: nagurney@hartford.edu

revised May 2012 and June 2012

*International Journal of Production Economics* **140(2)** (2012) pp 865-874.

**Abstract:** In this paper, we develop a tractable network model and computational approach for the design of medical nuclear supply chains. Our focus is on the molybdenum supply chain, which is the most commonly used radioisotope for medical imaging utilized in cardiac and cancer diagnostics. This topic is of special relevance to healthcare given the medical nuclear product's widespread use as well as the aging of the nuclear reactors where it is produced. The generalized network model, for which we derive formulae for the arc and path multipliers that capture the underlying physics of radioisotope decay, includes total operational cost minimization, and the minimization of cost associated with nuclear waste discarding, coupled with capacity investment costs. Its solution yields the optimal link capacities as well as the optimal product flows so that demand at the medical facilities is satisfied. We illustrate the framework with a case study. The framework provides the foundation for further empirical research and the basis for the modeling and analysis of supply chain networks for other very time-sensitive medical products.

**Keywords:** Supply chains, Nuclear medicine, Healthcare, Supply chain network design, Optimization, Variational inequalities, Generalized networks, Molybdenum, Time-sensitive products, Radioactive decay

\* corresponding author: phone: 413-545-5635; fax no.: 413-545-3858

## 1. Introduction

Medical nuclear supply chains are essential supply chains in healthcare and provide the conduits for products used in nuclear medical imaging, which is routinely utilized by physicians for diagnostic analysis. For example, each day, 41,000 nuclear medical procedures are performed in the United States using Technetium-99m, a radioisotope obtained from the decay of Molybdenum-99. Such supply chains have unique features and characteristics due to the products' time-sensitivity along with their hazardous nature. In this paper, we take on the challenge of developing a model for supply chain network design of medical nuclear products, which captures some of the salient issues surrounding such supply chains today, from their complexity, to the economic aspects, the underlying physics of radioactive decay, and the inclusion of waste management. We focus on Molybdenum-99 due to its importance in medical diagnostics, its time-sensitive nature, and the fact that there are only a handful of production and processing facilities for this radioisotope globally.

In order to appropriately ground our framework, we first describe the underlying features of medical nuclear supply chains, and provide the necessary background for their understanding. For example, to create an image for medical diagnostic purposes, a radioactive isotope is bound to a pharmaceutical that is injected into the patient and travels to the site or organ of interest. The gamma rays emitted by the radioactive decay of the isotope are then used to create an image of that site or organ (Berger, Goldsmith, and Lewis (2004)). Technetium,  $^{99m}Tc$ , which is a decay product of Molybdenum-99,  $^{99}Mo$ , is the most commonly used medical radioisotope, accounting for over 80% of the radioisotope injections and representing over 30 million procedures worldwide each year. Over 100,000 hospitals in the world use radioisotopes. (World Nuclear Association (2011)). In 2008, over 18.5 million doses of  $^{99m}Tc$  were injected in the US with 2/3 of them used for cardiac exams, with the other uses including bone scans, functional brain imaging, sentinel-node identification, immunoscintigraphy, blood pool labeling, pyrophosphates for identifying heart damage, and sulfure colloids for spleen scans (Lantheur Medical Imaging, Inc (2009)). Through this most widely used medical radioisotope, health professionals can enable the earlier and more accurate detection of cardiac problems as well as cancer, the two most common causes of death (see Kochanek et al. (2011)). It is estimated that the global market for medical isotopes is 3.7 billion US\$ per year (Kahn (2008)).

The production cycle of  $^{99m}\text{Tc}$ , typically, begins with the fission of Highly Enriched Uranium, HEU, to produce  $^{99}\text{Mo}$ , with a half-life of 66.7 hours. The  $^{99}\text{Mo}$ , in turn, decays to  $^{99m}\text{Tc}$ , whose half-life is approximately 6 hours. The relatively short half-life of  $^{99m}\text{Tc}$ , as compared to metabolism and human activity, makes it a suitable isotope for imaging. In addition, the gamma rays that are emitted due to the  $^{99m}\text{Tc}$  decay have roughly the same wavelength as common X-rays allowing detection by detectors similar to those used for medical x-rays.

The production of  $^{99}\text{Mo}$  occurs at only nine reactors in the world, with one in Canada, five in Europe, one in Australia, one in South Africa, and one in Argentina (see OECD (2010a)). The reactors irradiate targets, aluminum blocks or foil containing Uranium-235,  $^{235}\text{U}$ , to produce multiple fission products, including  $^{99}\text{Mo}$ . The irradiated targets containing the  $^{99}\text{Mo}$  are then shipped to processing facilities where the  $^{99}\text{Mo}$  is extracted and purified. The extracted  $^{99}\text{Mo}$  is further transported to generator manufacturing facilities. There, generators, which are containers of  $^{99}\text{Mo}$  in a chemical form that allows easy extraction of  $^{99m}\text{Tc}$  are produced. The generators, which are relatively radioactively safe, are then shipped to the hospitals and medical imaging facilities where the  $^{99m}\text{Tc}$  is eluted by a saline solution and the pharmaceutical injections prepared and administered. Since the decay of a single atom of  $^{99}\text{Mo}$  produces a single atom of  $^{99m}\text{Tc}$ , the activity of the generator is determined by the quantity of the  $^{99}\text{Mo}$  present.

Since  $^{99}\text{Mo}$  decays with a 66.7 hour half-life, approximately 99.9% of the atoms decay in 27.5 days, making its production, transportation, and processing all extremely time-sensitive. In fact, the production of  $^{99}\text{Mo}$  is quantified in *Six-day curies end of processing* denoting the activity of the sample 6 days after it was irradiated to highlight this (see OECD (2010a)). In addition to the time-sensitivity, the irradiated targets are highly radioactive, significantly constraining transportation options between the reactor and the processing facilities to only trucks that can transport the heavily shielded transportation containers. While the extracted  $^{99}\text{Mo}$  continues to be constrained by its decay, its shielding requirements are reduced, allowing for transportation by modes other than trucks, including by air (cf. de Lange (2010)).

Although the maximum possible production from current reactors in 2010 was well over

twice the current demand, it has been predicted that, with a 5% annual growth rate for imaging, the demand will exceed the supply by the end of the decade. However, this assumes that all reactors are capable of irradiating the necessary targets at all times. Due to routine maintenance, unexpected maintenance, and shutdowns due to safety concerns, the actual supply has been much closer to the demand. In 2009, in fact, the demand exceeded the supply and created a worldwide shortage of  $^{99}\text{Mo}$ . Furthermore, several of the reactors are reaching the end of their lifetimes, since they are 40 to over 50 years old (cf. OECD (2010a), Seeverens (2010)). Between 2000 and 2010, there were six unexpected shutdowns of reactors used for medical imaging products due to safety concerns (Ponsard (2010)) with the Canadian one shut down in May 2009 due to a leak in the reactor with its return to service more than a year later in August 2010.

It is also important to note that the number of processors that supply the global market is only four, and that they are located in Canada, Belgium, The Netherlands, and South Africa. Australia and Argentina produce bulk  $^{99}\text{Mo}$  for their domestic markets but are expected to export small amounts in the future. Amazingly, there are parts of the world in which there are no processing facilities for  $^{99}\text{Mo}$ , including the United States, parts of South America, and Japan. Such limitations in processing capabilities limit the ability to produce the medical radioisotopes from regional reactors since long-distance transportation of the product raises safety and security risks, and also results in greater decay of the product. The number of generator manufacturers, in turn, with substantial processing capabilities, is under a dozen (OECD (2010a)).

Furthermore, in 2016, the Canadian reactor is scheduled for complete shutdown, raising critical questions for supply chain network design, since its processing facility will also need to be shut down (OECD (2010a)).

This paper is organized as follows. In Section 2, we develop the multitiered supply chain network design model for Molybdenum,  $^{99}\text{Mo}$ . The framework may be used, with minor modification, for other radioisotopes. We describe the various tiers of the supply chain network, beginning with the nuclear reactors, moving on to the processors, then on to the generator manufacturing facilities, and, finally, to the hospitals and medical facilities, where the medical radioisotopes are injected into the patients. The supply chain network is quite

complex since it consists of multiple activities of production, transportation, and processing, coupled with the physics of the radioisotope and its decay, along with regulatory restrictions as to transportation, due to the hazardous nature of the medical nuclear product.

We model the supply chain network design problem as an optimization problem on a generalized network. We identify the specific losses on the links/arcs through the use of the time decay of the radioisotope. We consider total cost minimization associated with the operational costs, along with the waste management costs, since we are dealing with nuclear products. Medical nuclear waste management issues have not received much attention in recent reports (cf. OECD (2010a)). The model captures the investment in capacities through the construction of new links. Its solution provides the optimal investments along with the optimal levels of production, transportation, and processing, given the demands at the various hospitals and medical imaging facilities. We use a variational inequality formulation since such a formulation results in an elegant computational procedure. Moreover, the theory of variational inequalities has been applied to a plethora of supply chain modeling, analysis, and design problems (see Zhang (2006), Nagurney (2006, 2010), Qiang, Nagurney, and Dong (2009), Liu and Nagurney (2011), and Cruz and Liu (2011)). Furthermore, it provides a rigorous mathematical and computational framework to enable the exploration of alternative economic behaviors among the medical nuclear supply chain stakeholders, including competition (see Nagurney (2006)).

Such a modeling approach is in concert with recent studies that have focused on the security and reliability of medical nuclear supply chains that also emphasize that governments ultimately have the responsibility for establishing an environment conducive to investment in such supply chains (cf. OECD (2010a)). However, to the best of our knowledge, our model is the first mathematical one to include the operational, engineering, economic, and physics aspects of medical nuclear products. Indeed, the model is sufficiently general to capture the economic aspects of medical nuclear supply chain network design, which is an important issue since it has been recognized that usually governments run the reactors, which are research reactors, and the prices associated with the radioisotope may fail to capture the associated costs and, as a consequence, the pricing may be below marginal costs resulting in market failure; see OECD (2010a) and Seeverens (2010). For references to other generalized nonlinear network models and applications, see Nagurney and Aronson (1989), Nagurney,

Masoumi, and Yu (2012), and the references therein. Nagurney and Masoumi (2012) recently developed a supply chain network design model for a sustainable blood banking system but the demands therein were uncertain. In our model and applications the demands are fixed since the associated medical procedures need to be scheduled.

In Section 3, we propose a computational approach for the new model, along with the accompanying theory, which resolves the supply chain network design problem into subproblems that can be solved explicitly and exactly at each iteration. In Section 4, we present a case study. In Section 5, we summarize our findings, present our conclusions, and provide suggestions for future research.

## 2. The Medical Nuclear Supply Chain Network Design Model

In this Section, we develop the supply chain network design model for a medical nuclear product, that of  $^{99}Mo$ , referred to, henceforth, as  $Mo$ . The model is general and can be applied, with appropriate data, to evaluate the design of such supply chains in the cognizant organization's nation / region. In Section 4, we illustrate how this framework can be applied to the Canada - United States and other countries supply chain for this product.

For definiteness, please refer to Figure 1. Figure 1 depicts a possible network topology of the medical nuclear supply chain. In this network, the top level (origin) node 0 represents the organization and the bottom level nodes represent the destination nodes. Every other node in the network denotes a component/facility in the system. A path connecting the origin node to a destination node, corresponding to a demand point, consists of a sequence of directed links which correspond to supply chain network activities that ensure that the nuclear product is produced, processed, and, ultimately, distributed to the hospitals and medical imaging facilities, where they are administered to the patients. We assume that, in the initial supply chain network topology, as in Figure 1, which serves as a template upon which the optimal supply chain network design is constructed, there exists at least one path joining node 0 with each destination node:  $H_1^2, \dots, H_{n_H}^2$ . This assumption guarantees that the demand at each demand point will be met.

The solution of the model yields the optimal investments associated with the various links as well as the optimal flows, at minimum total cost, as we shall demonstrate, and, hence,

the optimal medical nuclear product supply chain network design.

In the network in Figure 1, we assume that the organization is considering  $n_R$  possible reactor sites, which produce the radioisotope. These are usually government research reactors and constitute the second tier of nodes of the network:  $R_1, R_2, \dots, R_{n_R}$ . The first set of links, connecting the origin node to the second tier, corresponds to the process of radioisotope production.

The next set of nodes, located in the third tier, consists of the radioisotope processing centers. There exist, potentially,  $n_C$  of these facilities, denoted, respectively, by  $C_1^1, C_2^1, \dots, C_{n_C}^1$ , to which the *Mo* is shipped after being produced at the reactor sites. Thus, the next set of links connecting tiers two and three of the network topology represents the transportation of the radioisotope. Transportation at this stage of the radioisotope, which is a hazardous material, is done exclusively by a single mode of transportation, that is, by truck, using specialized containers. Note that the single mode of transportation is represented by single links joining the pairs of nodes. Hence, the processing facilities must be located fairly near to the reactors since the transportation is done by land. At these processing centers, the *Mo* is extracted and purified. This processing is represented by the links emanating from the nodes:  $C_1^1, C_2^1, \dots, C_{n_C}^1$  and ending in the nodes:  $C_1^2, C_2^2, \dots, C_{n_C}^2$ , with the latter set of nodes being the fourth tier nodes.

The fifth tier of the network is associated with the generator manufacturing facilities, and these nodes are joined with the fourth tier nodes by links which represent the multiple modes of transportation that are being considered for transporting the purified *Mo* to the generator manufacturing facilities. The number of these potential generator manufacturing facilities is given by  $n_G$ . These facilities are denoted by  $G_1^1, \dots, G_{n_G}^1$ , respectively, and need not be located near the processing facilities. The generator manufacturing facilities are further involved in the processing of the radioisotopes, through the production of the generators that contain them, and the links that emanate from the generator manufacturing facility nodes terminate in the sixth tier set of nodes, respectively, denoted by  $G_1^2, \dots, G_{n_G}^2$  in Figure 1, which represent the completion of this stage of processing.

From the latter generator nodes, there emanate a variety of possible transportation links and these links, as the preceding transportation links, correspond to multiple modes of

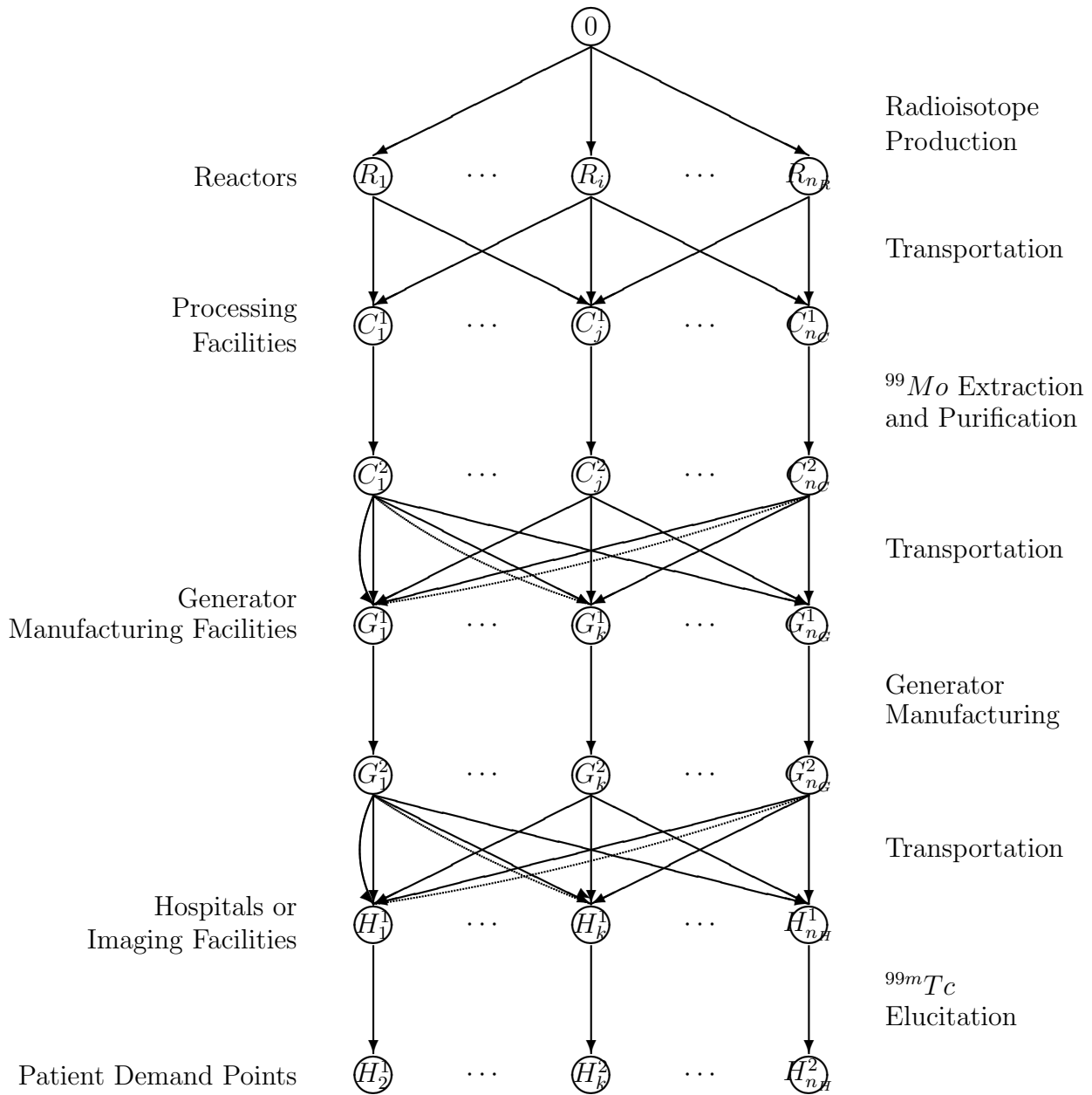


Figure 1: The Medical Nuclear Supply Chain Network Topology

transportation, as appropriate, including not only trucking but also air transportation, if appropriate. These links terminate in the seventh tier of nodes,  $H_1^1, \dots, H_{n_H}^1$ , which represent the hospitals and the medical facilities that dispense the radioisotope to the patients. There is still one more stage of processing, however, represented by the final set of links in Figure 1, terminating in nodes:  $H_1^2, \dots, H_{n_H}^2$ , which represent the final patient demand points.

The possible supply chain network topology, as depicted in Figure 1, is represented by  $\mathcal{G} = [N, L]$ , where  $N$  and  $L$  denote the sets of nodes and links, respectively. The ultimate solution of the complete model will yield the optimal capacities on the various links of the network as well as the optimal flows.

The formalism that we utilize is that of generalized network optimization, where the organization seeks to minimize the total costs associated with the production, processing, and transportation activities, along with the total investment corresponding to the construction of the links from scratch, as well as the total cost of discarding the associated nuclear waste product associated with the links.

We assume that the demands must be satisfied since we are dealing with a healthcare product. This assumption is appropriate since the radioisotope-utilizing procedures tend to be scheduled in advance.

With each link of the network, we associate a unit operational cost function that reflects the cost of operating the particular supply chain activity. The links are denoted by  $a, b$ , etc. The unit operational cost on link  $a$  is denoted by  $c_a$  and is a function of flow on that link,  $f_a$ . The *total* operational cost on link  $a$  is denoted by  $\hat{c}_a$ , and is constructed as:

$$\hat{c}_a(f_a) = f_a \times c_a(f_a), \quad \forall a \in L. \quad (1)$$

The link total cost functions are assumed to be convex and continuously differentiable.

Let  $w_k$  denote the pair of origin/destination (O/D) nodes  $(0, H_k^2)$  and let  $\mathcal{P}_{w_k}$  denote the set of paths, which represent the alternative associated possible supply chain network processes, joining  $(0, H_k^2)$ .  $\mathcal{P}$  denotes the set of all paths joining node 0 to the destination nodes, and  $n_{\mathcal{P}}$  denotes the number of paths.

Let  $d_k$  denote the demand for the radioisotope at the demand point  $H_k^2$ ;  $k = 1, \dots, n_H$ .

We associate with every link  $a$  in the network, a multiplier  $\alpha_a$ , which corresponds to the percentage of decay and additional loss over that link. This multiplier lies in the range  $(0,1]$ , for the network activities, where  $\alpha_a = 1$  means that 100% of the initial flow on link  $a$  reaches the successor node of that link, reflecting that there is no decay/waste/loss on link  $a$ . The multiplier  $\alpha_a$  can be modeled as the product of two terms, a radioactive decay multiplier  $\alpha_{da}$  and a processing loss multiplier  $\alpha_{la}$ , which we discuss how to obtain below.

### Capturing the Underlying Physics Through Link and Path Multipliers

The activity of a radioisotope (in disintegrations per unit time) is proportional to the quantity of that isotope, i.e.,

$$\frac{dN}{dt} \propto N, \quad (2)$$

where  $N = N(t)$  = the quantity of a radioisotope. The quantity of a radioisotope in a time interval  $t$  is then given by

$$N(t) = N_0 e^{-\lambda t}, \quad (3)$$

where  $N_0$  is the quantity present at the beginning of the interval and  $\lambda$  is the decay constant of the radioisotope (see Berger, Goldsmith, and Lewis (2004)).

Hence, we can represent the radioactive decay multiplier  $\alpha_{da}$  for link  $a$  as

$$\alpha_{da} = e^{-\lambda t_a}, \quad (4)$$

where  $t_a$  is the time spent on the link  $a$ . The decay constant,  $\lambda$ , in turn, can be conveniently represented by an experimentally measured value, called the half-life  $t_{1/2}$ , where

$$t_{1/2} = \frac{\ln 2}{\lambda}. \quad (5)$$

The values of the half-lives of radioisotopes are tabulated in the American Institute of Physics Handbook (1972). Thus, we can write  $\alpha_{da}$  as

$$\alpha_{da} = e^{-\lambda t_a} = e^{-\ln 2 \frac{t_a}{t_{1/2}}} = 2^{-\frac{t_a}{t_{1/2}}}. \quad (6)$$

The value of  $t_{1/2}$  for  $Mo$ , as noted in the Introduction, is 66.7 hours. If one is interested in another radioisotope, then the arc multiplier can be computed accordingly using that radioisotope's half-life.

The processing loss multiplier  $\alpha_{la}$  for link  $a$ , in turn, is a factor in the range  $(0,1]$  that quantifies for the losses that occur during processing. Different processing links may have different values for this parameter. For transportation links, however, there is no loss beyond that due to radioactive decay; therefore,  $\alpha_{la} = 1$  for such links. For the top-most manufacturing links  $\alpha_a = 1$ .

As mentioned earlier,  $f_a$  denotes the (initial) flow on link  $a$ . Let  $f'_a$  denote the final flow on that link; i.e., the flow that reaches the successor node of the link. Therefore,

$$f'_a = \alpha_a f_a, \quad \forall a \in L. \quad (7)$$

The organization is also responsible for disposing the waste which is hazardous.

Since  $\alpha_a$  is constant, and known apriori, a total discarding cost function,  $\hat{z}_a$ , can be defined accordingly, which is a function of the flow,  $f_a$ , and is assumed to be convex and continuously differentiable and given by:

$$\hat{z}_a = \hat{z}_a(f_a), \quad \forall a \in L. \quad (8)$$

Note that, in processing/producing an amount of radioisotope  $f_a$ , one knows from the physics the amount of hazardous waste and, hence, a discarding function of the form (8) is appropriate.

Let  $x_p$  represent the (initial) flow of  $Mo$  on path  $p$  joining the origin node with a destination node. The path flows must be nonnegative, that is,

$$x_p \geq 0, \quad \forall p \in \mathcal{P}, \quad (9)$$

since the nuclear product will be produced, processed, transported, etc., in nonnegative quantities.

Let  $\mu_p$  denote the multiplier corresponding to the loss on path  $p$ , which is defined as the

product of all link multipliers on links comprising that path, that is,

$$\mu_p \equiv \prod_{a \in p} \alpha_a, \quad \forall p \in \mathcal{P}. \quad (10)$$

The demand at demand point  $R_k$ ,  $d_k$ , is the sum of all the final flows on paths joining  $(0, H_k^2)$ :

$$d_k \equiv \sum_{p \in \mathcal{P}_{w_k}} \mu_p x_p, \quad k = 1, \dots, n_H. \quad (11)$$

Indeed, although the amount of radioisotope that originates on a path  $p$  is  $x_p$ , the amount (due to radioactive decay, etc.) that actually arrives at the destination (terminal node) of this path is  $x_p \mu_p$ .

The multiplier  $\alpha_{ap}$  is the product of the multipliers of the links on path  $p$  that precede link  $a$  in that path. This multiplier can be expressed as:

$$\alpha_{ap} \equiv \begin{cases} \delta_{ap} \prod_{a' < a} \alpha_{a'}, & \text{if } \{a' < a\} \neq \emptyset, \\ \delta_{ap}, & \text{if } \{a' < a\} = \emptyset, \end{cases} \quad (12)$$

where  $\{a' < a\}$  denotes the set of the links preceding link  $a$  in path  $p$ , and  $\delta_{ap}$  is defined as equal to one if link  $a$  is contained in path  $p$ ; otherwise, it is equal to zero, and  $\emptyset$  denotes the null set. In other words,  $\alpha_{ap}$  is equal to the product of all link multipliers preceding link  $a$  in path  $p$ . If link  $a$  is not contained in path  $p$ , then  $\alpha_{ap}$  is set to zero. The relationship between the link flow,  $f_a$ , and the path flows is as follows:

$$f_a = \sum_{p \in \mathcal{P}} x_p \alpha_{ap}, \quad \forall a \in L. \quad (13)$$

The organization wishes to determine which facilities should operate and at what level, with the demand being satisfied, and the total cost being minimized. Let  $\bar{u}_a$  denote the nonnegative existing capacity on link  $a$ ,  $\forall a \in L$ . The organization can enhance/reduce the capacity of link  $a$  by  $u_a$ ,  $\forall a \in L$ . The total investment cost of adding capacity  $u_a$  on link  $a$ , is denoted by  $\hat{\pi}_a$ , and is a function of the capacity:

$$\hat{\pi}_a = \hat{\pi}_a(u_a), \quad \forall a \in L. \quad (14)$$

These functions are also assumed to be convex and continuously differentiable. Such an assumption is reasonable since the units for the variable  $u_a$ ,  $a \in L$  are in amounts of the material being processed on that link, for consistency in our model, and as is common accounting practice. Note that the amortization of the investment capacity costs on the links may take place over different time scales. However, the form in (14) is over days, which is the scale of time for this product's production, delivery, and ultimate use. At low levels of material, the investment costs are expected to be high, gradually decreasing until a region where the investment costs will increase because of additional capacity required. In addition, the capacity investments are functions of continuous amounts of material being processed. See also OECD (2010b).

We group the link capacities into the vector  $u$ . The path flows and the link flows, in turn, are grouped into the respective vectors:  $x$  and  $f$ .

The total cost minimization objective faced by the organization includes the total cost of operating the various links, the total discarding cost of waste/loss over the links, and the total cost of the capacities. This optimization problem can be expressed as:

$$\text{Minimize } \sum_{a \in L} \hat{c}_a(f_a) + \sum_{a \in L} \hat{z}_a(f_a) + \sum_{a \in L} \hat{\pi}_a(u_a) \quad (15)$$

subject to: constraints (9), (11), and (13), and

$$f_a \leq u_a, \quad \forall a \in L, \quad (16)$$

$$0 \leq u_a, \quad \forall a \in L. \quad (17)$$

Constraint (16) guarantees that the flow on a link cannot exceed the capacity on that link. Constraint (17), in turn, guarantees that the flow on a link will not be negative (see Nagurney (2010)). It is important to recognize that the enhancement in capacities is reflected in the additional amount of radioactive material that can be processed.

The above optimization problem is in terms of link flows. It can also be expressed, in view of (13), in terms of path flows:

$$\text{Minimize } \sum_{p \in \mathcal{P}} (\hat{C}_p(x) + \hat{Z}_p(x)) + \sum_{a \in L} \hat{\pi}_a(u_a) \quad (18)$$

subject to: constraints (9), (11), (17), and (16), but with the  $f_a$  in (16) being replaced by its expression in (13), with the total operational cost function,  $\hat{C}_p(x)$ , and the total discarding cost function,  $\hat{Z}_p(x)$ , corresponding to path  $p$ , respectively, derived from  $C_p(x)$ , and  $Z_p(x)$  as follows:

$$\begin{aligned}\hat{C}_p(x) &= x_p \times C_p(x), & \forall p \in \mathcal{P}_{w_k}; k = 1, \dots, n_H, \\ \hat{Z}_p(x) &= x_p \times Z_p(x), & \forall p \in \mathcal{P}_{w_k}; k = 1, \dots, n_H.\end{aligned}\tag{19}$$

with the unit cost functions on path  $p$ , i.e.,  $C_p(x)$ ,  $Z_p(x)$ , and  $R_p(x)$ , in turn, defined as:

$$\begin{aligned}C_p(x) &\equiv \sum_{a \in L} c_a(f_a) \alpha_{ap}, & \forall p \in \mathcal{P}_{w_k}; k = 1, \dots, n_H, \\ Z_p(x) &\equiv \sum_{a \in L} z_a(f_a) \alpha_{ap}, & \forall p \in \mathcal{P}_{w_k}; k = 1, \dots, n_H.\end{aligned}\tag{20}$$

We associate the Lagrange multiplier  $\gamma_a$  with constraint (16) for each link  $a$ , and we denote the optimal Lagrange multiplier by  $\gamma_a^*$ ,  $\forall a \in L$ . The Lagrange multipliers may be interpreted as shadow prices. We group these Lagrange multipliers into the vector  $\gamma$ .

Let  $K$  denote the feasible set such that:

$$K \equiv \{(x, u, \gamma) | x \in R_+^{n_P}, (11) \text{ and } (17) \text{ hold, and } \gamma \in R_+^{n_L}\}.\tag{21}$$

Before stating the variational inequality formulation of the problem, we recall a lemma that formalizes the construction of the partial derivatives of the total operational cost and the total discarding cost with respect to a path flow. This lemma was derived for another time-sensitive product supply chain in healthcare – that of human blood. However, in that application the arc and path multipliers have an entirely different meaning than that in the case of medical nuclear products.

### Lemma

*The partial derivatives of the total operational cost and the total discarding cost, with respect to a path flow are, respectively, given by:*

$$\frac{\partial(\sum_{q \in \mathcal{P}} \hat{C}_q(x))}{\partial x_p} \equiv \sum_{a \in L} \frac{\partial \hat{c}_a(f_a)}{\partial f_a} \alpha_{ap}, \quad \forall p \in \mathcal{P}_{w_k}; k = 1, \dots, n_H,$$

$$\frac{\partial(\sum_{q \in \mathcal{P}} \hat{Z}_q(x))}{\partial x_p} \equiv \sum_{a \in L} \frac{\partial \hat{z}_a(f_a)}{\partial f_a} \alpha_{ap}, \quad \forall p \in \mathcal{P}_{w_k}; k = 1, \dots, n_H. \quad (22)$$

**Proof:** See Nagurney, Masoumi, and Yu (2012) for the proof.

We now derive the variational inequality formulations of the problem in terms of path flows and link flows.

### Theorem: Variational Inequality Formulations

The optimization problem (18), subject to its constraints, is equivalent to the variational inequality problem: determine the vector of optimal path flows, the vector of optimal capacities, and the vector of optimal Lagrange multipliers  $(x^*, u^*, \gamma^*) \in K$ , such that:

$$\begin{aligned} & \sum_{k=1}^{n_R} \sum_{p \in \mathcal{P}_{w_k}} \left[ \frac{\partial(\sum_{q \in \mathcal{P}} \hat{C}_q(x^*))}{\partial x_p} + \frac{\partial(\sum_{q \in \mathcal{P}} \hat{Z}_q(x^*))}{\partial x_p} + \sum_{a \in L} \gamma_a^* \alpha_{ap} \right] \times [x_p - x_p^*] \\ & + \sum_{a \in L} \left[ \frac{\partial \hat{\pi}_a(u_a^*)}{\partial u_a} - \gamma_a^* \right] \times [u_a - u_a^*] + \sum_{a \in L} \left[ u_a^* - \sum_{p \in \mathcal{P}} x_p^* \alpha_{ap} \right] \times [\gamma_a - \gamma_a^*] \geq 0, \forall (x, u, \gamma) \in K. \end{aligned} \quad (23)$$

Variational inequality (23), in turn, can be rewritten in terms of link flows as: determine the vector of optimal link flows, the vector of the link capacity adjustments, and the vector of optimal Lagrange multipliers  $(f^*, u^*, \gamma^*) \in K^1$ , such that:

$$\begin{aligned} & \sum_{a \in L} \left[ \frac{\partial \hat{c}_a(f_a^*)}{\partial f_a} + \frac{\partial \hat{z}_a(f_a^*)}{\partial f_a} + \gamma_a^* \right] \times [f_a - f_a^*] + \sum_{a \in L} \left[ \frac{\partial \hat{\pi}_a(u_a^*)}{\partial u_a} - \gamma_a^* \right] \times [u_a - u_a^*] \\ & + \sum_{a \in L} [u_a^* - f_a^*] \times [\gamma_a - \gamma_a^*] \geq 0, \quad \forall (f, u, \gamma) \in K^1, \end{aligned} \quad (24)$$

where  $K^1$  denotes the feasible set:

$$K^1 \equiv \{(f, u, \gamma) | \exists x \geq 0, (11), (13), (17) \text{ hold, and } \gamma \geq 0\}. \quad (25)$$

**Proof:** First, we prove the result for path flows (cf. (23)).

The convexity of  $\hat{C}_p$  and  $\hat{Z}_p$  for all paths  $p$  holds since  $\hat{c}_a$  and  $\hat{z}_a$  were assumed to be convex for all links  $a$ . The convexity of  $\hat{\pi}_a$  was also assumed to hold and, as a consequence, the objective function in (23) is also convex.

Since the objective function (23) is convex and the feasible set  $K$  is closed and convex, the variational inequality (23) follows from the standard theory of variational inequalities (see Nagurney (1999)).

As for the proof of the variational inequality (24), now that (23) is established, we can apply the equivalence between partial derivatives of total costs on paths and partial derivatives of total costs on links from Lemma 1. Also, using (13) and (16), we can rewrite the formulation in terms of link flows rather than path flows. Thus, the second part of Theorem 1, that is, the variational inequality in link flows (24), also holds.

Variational inequality (23) can be put into standard form VI  $(F, \mathcal{K})$  (see Nagurney (1999)) as follows: determine  $X^* \in \mathcal{K}$  such that:

$$\langle F(X^*)^T, X - X^* \rangle \geq 0, \quad \forall X \in \mathcal{K}, \quad (26)$$

where  $\langle \cdot, \cdot \rangle$  denotes the inner product in  $n$ -dimensional Euclidean space.

If we define the feasible set  $\mathcal{K} \equiv K$ , and the column vector  $X \equiv (x, u, \gamma)$ , and  $F(X) \equiv (F_1(X), F_2(X), F_3(X))$ , where:

$$\begin{aligned} F_1(X) &= \left[ \frac{\partial(\sum_{q \in \mathcal{P}} \hat{C}_q(x))}{\partial x_p} + \frac{\partial(\sum_{q \in \mathcal{P}} \hat{Z}_q(x))}{\partial x_p} + \sum_{a \in L} \gamma_a \alpha_{ap}; p \in \mathcal{P}_{w_k}; k = 1, \dots, n_H \right], \\ F_2(X) &= \left[ \frac{\partial \hat{\pi}_a(u_a)}{u_a} - \gamma_a; \quad a \in L \right], \\ F_3(X) &= \left[ u_a - \sum_{p \in \mathcal{P}} x_p \alpha_{ap}; \quad a \in L \right], \end{aligned} \quad (27)$$

then variational inequality (23) can be re-expressed in standard form (26).

We will utilize variational inequality (23) in path flows for the proposed computational approach.

### 3. The Computational Approach

In this section, we propose the computational approach for the solution of our novel medical nuclear supply chain network design model. Specifically, we propose the modified projection method, but in path flows, rather than in link flows (see, e.g., Nagurney and Qiang (2009) Liu and Nagurney (2011), and references therein). This algorithm, in the context of our new model, yields subproblems, as we show below, that can be solved exactly, and in closed form, using a variant of the exact equilibration algorithm, adapted to handle the arc/path multipliers, and by applying explicit formulae for the capacity investments and for the Lagrange multipliers.

The modified projection is guaranteed to converge if the function  $F$  that enters the variational inequality satisfies monotonicity and Lipschitz continuity (see Nagurney (1999)).

We now recall the modified projection method, where  $\mathcal{T}$  denotes an iteration counter.

#### Step 0: Initialization

Set  $X^0 \in \mathcal{K}$ . Let  $\mathcal{T} = 1$  and let  $\eta$  be a scalar such that  $0 < \eta \leq \frac{1}{L}$ , where  $L$  is the Lipschitz continuity constant.

#### Step 1: Computation

Compute  $\tilde{X}^{\mathcal{T}}$  by solving the VI subproblem:

$$\langle \tilde{X}^{\mathcal{T}} + \eta F(X^{\mathcal{T}-1}) - X^{\mathcal{T}-1}, X - \tilde{X}^{\mathcal{T}} \rangle \geq 0, \quad \forall X \in \mathcal{K}. \quad (28)$$

#### Step 2: Adaptation

Compute  $X^{\mathcal{T}}$  by solving the VI subproblem:

$$\langle X^{\mathcal{T}} + \eta F(\tilde{X}^{\mathcal{T}}) - X^{\mathcal{T}-1}, X - X^{\mathcal{T}} \rangle \geq 0, \quad \forall X \in \mathcal{K}. \quad (29)$$

#### Step 3: Convergence Verification

If  $\max |X_l^{\mathcal{T}} - X_l^{\mathcal{T}-1}| \leq \epsilon$ , for all  $l$ , with  $\epsilon > 0$ , a prespecified tolerance, then stop; else, set  $\mathcal{T} =: \mathcal{T} + 1$ , and go to Step 1.

The VI subproblems in (28) and (29) are quadratic programming problems with special structure that result in straightforward computations. Explicit formulae for (28) for the supply chain network problem are now given for the capacity investments and the Lagrange multipliers. Analogous formulae for (29) can then be easily obtained. Subsequently, we follow up with how the path flow values for (28) can be determined (a similar approach can then be used to determine the path flows for (29)).

**Explicit Formulae for the Investment Capacities and the Lagrange Multipliers at Step 1 (cf. (28))**

$$\tilde{u}_a^T = \max\{0, u_a^{T-1} + \eta(\gamma_a^{T-1} - \frac{\partial \hat{\pi}_a(u_a^{T-1})}{\partial u_a})\}, \quad \forall a \in L; \quad (30)$$

$$\tilde{\gamma}_a^T = \max\{0, \gamma_a^{T-1} + \eta(\sum_{p \in \mathcal{P}} x_p^{T-1} \alpha_{ap} - u_a^{T-1})\}, \quad \forall a \in L. \quad (31)$$

Recall that the feasible set  $\mathcal{K}$ , in terms of the path flows, requires that the path flows be nonnegative and that the demand constraint (11) holds for each demand point. The induced path flow subproblems in (28) and (29), hence, have a special network structure of the form given in Figure 2.

Specifically, the path flow subproblems that one must solve in Step 1 (see (28)) (we have suppressed the iteration superscripts below) have the following form for each demand point  $k$ ;  $k = 1, \dots, n_H$ :

$$\text{Minimize } \frac{1}{2} \sum_{p \in \mathcal{P}_{w_k}} x_p^2 + \sum_{p \in \mathcal{P}_{w_k}} h_p x_p \quad (32)$$

subject to:

$$d_k \equiv \sum_{p \in \mathcal{P}_{w_k}} \mu_p x_p, \quad (33)$$

$$x_p \geq 0, \quad \forall p \in \mathcal{P}_{w_k}, \quad (34)$$

where  $h_p \equiv -x_p^{T-1} + \eta \left[ \frac{\partial(\sum_{q \in \mathcal{P}} \hat{C}_q(x^{T-1}))}{\partial x_p} + \frac{\partial(\sum_{q \in \mathcal{P}} \hat{Z}_q(x^{T-1}))}{\partial x_p} + \sum_{a \in L} \gamma_a^{T-1} \alpha_{ap} \right]$ .

We now present an exact equilibration algorithm, adapted to handle the multipliers, which can be applied to compute the solution to problem (32), for each demand point, subject to

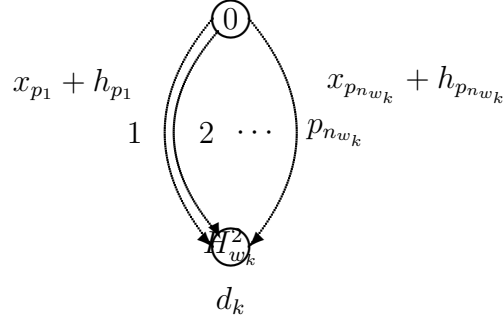


Figure 2: Special Network Structure of an Induced Path Flow Subproblem for Each Demand Point  $k$

constraints (33) and (34). An analogous set of subproblems in path flows can be set up and solved accordingly for Step 2 (cf. (29)). For further background on such algorithms, see Nagurney and Qiang (2009) and the references therein.

### An Exact Equilibration Algorithm for a Generalized Specially Structured Network

#### Step 0: Sort

Sort the fixed terms  $h_p$ ;  $p \in \mathcal{P}_{w_k}$  in nondescending order and relabel the paths/links accordingly. Assume, from this point on, that they are relabeled. Set  $h_{p_{n_{w_k}+1}} \equiv \infty$ , where  $n_{w_k}$  denotes the number of paths connecting destination node  $H_k^2$  with origin node 0. Set  $r = 1$ .

#### Step 1: Computation

Compute

$$\lambda_k^r = \frac{\sum_{i=1}^r \mu_{p_i} h_{p_i} + d_k}{\sum_{i=1}^r \mu_{p_i}^2}. \quad (35)$$

#### Step 2: Evaluation

If  $h_{p_r} < \lambda_k^r \leq h_{p_{r+1}}$ , then stop; set  $s = r$  and go to Step 3; otherwise, let  $r = r + 1$  and return

to Step 1.

### Step 3: Path Flow Determination

Set

$$\begin{aligned} x_{p_i} &= \lambda_k^s - h_{p_i}, \quad i = 1, \dots, s. \\ x_{p_i} &= 0, \quad i = s + 1, \dots, n_{w_k}. \end{aligned} \tag{36}$$

In summary, the proposed computational procedure, at Steps 1 and 2 (see (28) and (29)), induces subproblems of special structure, each of which can be solved explicitly and in closed form. For the induced subproblems in capacities and Lagrange multipliers, we have provided the formulae (28) and (29), whereas for the induced subproblems in the path flows, we have provided a variant of the exact equilibration algorithm to handle the multipliers.

The modified projection method is guaranteed to converge to a solution of the medical nuclear supply chain network design problem provided that the function  $F$  (cf. (26) and (27)) is monotone and Lipschitz continuous. Monotonicity follows under our imposed assumptions and Lipschitz continuity will also hold provided that the marginal total cost and marginal risk functions have bounded second order partial derivatives.

## 4. A Case Study

In this section, we describe a case study. In particular, we consider the Molybdenum-99 supply chain in North America with the focus on the Canadian reactor, the Canadian processing facility, and the two US generator manufacturing facilities. This reactor is to be decommissioned around 2016; the same holds for the processing facility.

The existing supply chain is as depicted in Figure 3.

The reactor, known as NRU, is located in Chalk River, Ontario. The processing facility is located in Ottawa, and is known as AECL-MDS Nordion. Transportation of the irradiated targets from NRU to AECL - MDS Nordion takes place by truck. There are two generator manufacturers in the United States (and none in Canada). The two existing generator manufacturers are located in Billerica, Massachusetts and outside of St. Louis, Missouri.

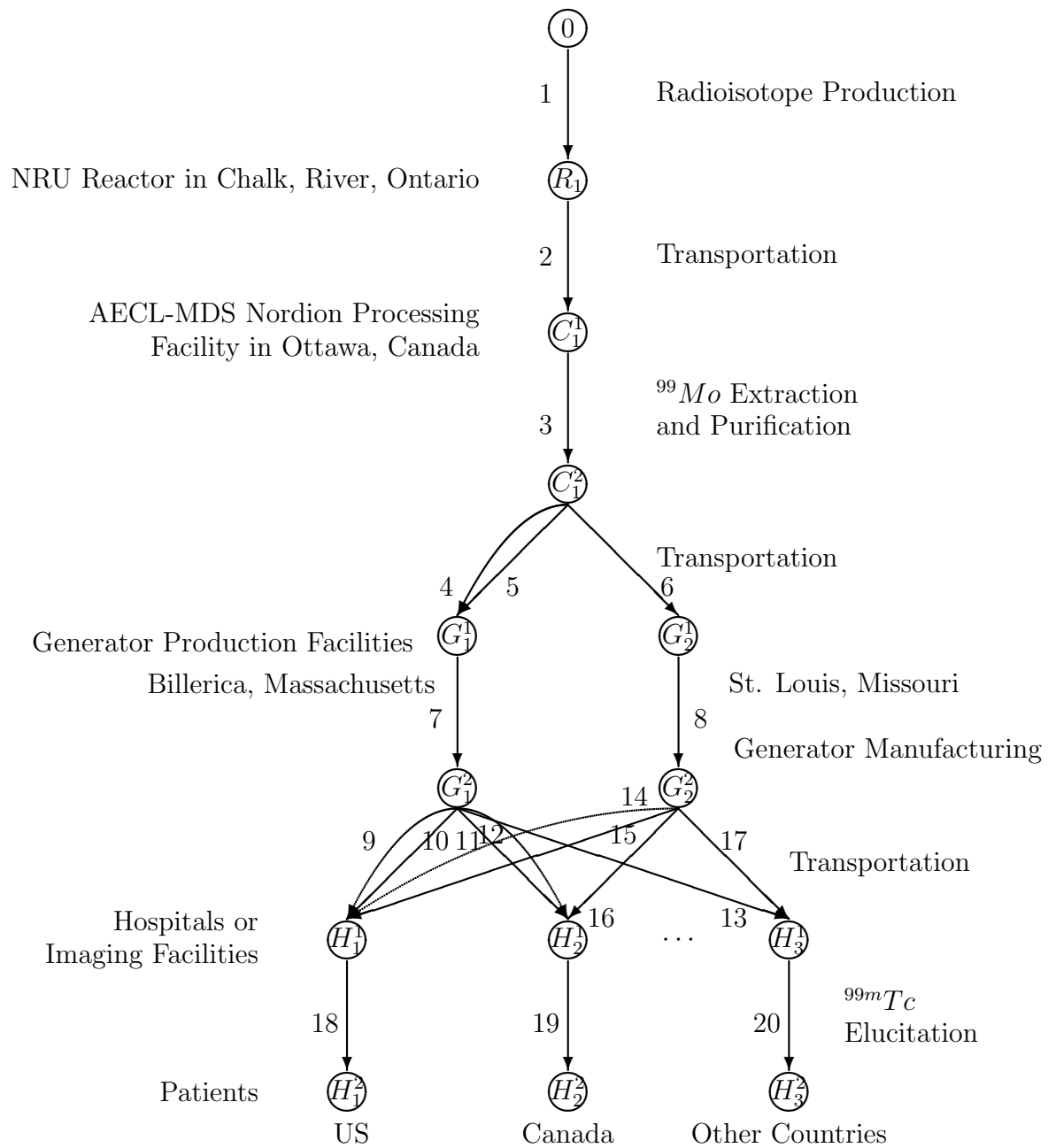


Figure 3: The Existing Supply Chain Topology for MO-99 from Canada to the United States, Canada, and Other Countries

In this case study, we utilized the supply chain network in Figure 3 as a template.

We implemented the modified projection method, along with the generalized exact equilibration algorithm, as described in Section 3 for the solution of our supply chain network design problem. The  $\epsilon$  in the convergence criterion was  $10^{-6}$ . The algorithm was implemented in FORTRAN and a Unix-based system at the University of Massachusetts was used for the computations.

The arc multipliers, the total operational cost functions, the total discarding cost functions, and the total capacity investment cost functions, and the optimal link flow and capacity solutions are reported in Table 1. Links 4, 6, 9,12,13,14, and 16 correspond to transportation by air, whereas links 5, 10, 11, and 15 correspond to transportation by truck. We calculated the values of the arc multipliers  $\alpha_{da}$ , for all links  $a = 1, \dots, 20$ , using data in the OECD (2010a) report and in the National Research Council (2009) report, which included the approximate times associated with the various links in the supply chain network in Figure 3. According to OECD (2010a), we may assume that there is no loss  $a_{la}$  on each link  $a$  for  $a = 1, \dots, 20$ , except for processing link 3; hence,  $\alpha_{la} = 1$  for all the former links; therefore,  $\alpha_a = \alpha_{da}$  for all those links, as reported in Table 1. In the case of link 3,  $\alpha_{la} = .8$  and  $\alpha_{da} = .883$ ; therefore,  $\alpha_3 = .706$ . All capacities and flows are reported in Curies.

Capital and operating cost data were taken from OECD (2010b) and converted to per Curie processed or generated. As noted by the National Research Council (2009), the US generator prices are proprietary, but could be estimated from a functional form derived from publicly available prices for Australian generators coupled with several spot prices for US made generators.

We assumed three demand points corresponding, respectively, to the collective demands in the US, in Canada, and in other countries (such as Mexico, and the Caribbean Islands). We are using 3 demand points, as approximations, in order to be able to report the input and output data for transparency purposes. The demands were as follows:  $d_1 = 3,600$ ,  $d_2 = 1,800$ , and  $d_3 = 1,000$  and these denote the demands, in Curies, per week. These values were obtained by using the daily number of procedures in the US and extrapolating for the others. The units for the path and link flows are also Curies. We have chosen to include 3 demand points since, within the US, the shipping times between the generator

Table 1: Link Multipliers, Total Operational Cost, Total Discarding Cost, and Total Capacity Investment Cost Functions and Optimal Link Flow and Capacity Solution for Example 1

Link $a$	$\alpha_a$	$\hat{c}_a(f_a)$	$\hat{z}_a(f_a)$	$\hat{\pi}_a(u_a)$	$f_a^*$	$u_a^*$
1	1.00	$2f_1^2 + 25.6f_1$	0.00	$u_1^2 + 743u_1$	15,034	15,034
2	.969	$f_2^2 + 5f_2$	0.00	$.5u_2^2 + u_2$	15,034	15,034
3	.706	$5f_3^2 + 192f_3$	$5f_3^2 + 80f_3$	$.5u_3^2 + 289u_3$	14,568	14,568
4	.920	$2f_4^2 + 4f_4$	0.00	$.5u_4^2 + 4u_4$	4,254	4,253
5	.901	$f_5^2 + f_5$	0.00	$2.5u_5^2 + 2u_5$	1,286	1,286
6	.915	$f_6^2 + 2f_6$	0.00	$.5u_6^2 + u_6$	4,744	4,744
7	.804	$f_7^2 + 166f_7$	$2f_7^2 + 7f_7$	$.5u_7^2 + 289u_7$	5,072	5,072
8	.804	$f_8^2 + 166f_8$	$2f_7^2 + 7f_7$	$.5u_8^2 + 279u_8$	4,341	4,341
9	.779	$2f_9^2 + 4f_9$	0.00	$.5u_3^2 + 3u_9$	0.00	0.00
10	.883	$f_{10}^2 + 1f_{10}$	0.00	$.5u_{10}^2 + 5u_{10}$	2,039	2,039
11	.883	$2f_{11}^2 + 4f_{11}$	0.00	$.5u_{11}^2 + 3u_{11}$	2,039	2,039
12	.688	$f_{12}^2 + 2f_{12}$	0.00	$.5u_{12}^2 + f_{12}$	0.00	0.00
13	.688	$2.5f_{13}^2 + 2f_{13}$	0.00	$.5f_{13}^2 + u_{13}$	0.00	0.00
14	.779	$2f_{14}^2 + 2f_{14}$	0.00	$u_{14}^2 + uf_{14}$	0.00	0.00
15	.883	$f_{15}^2 + 7f_{15}$	0.00	$2u_{15}^2 + 5u_{15}$	2,037	2,037
16	.688	$2f_{16}^2 + 4f_{16}$	0.00	$.5u_{16}^2 + u_{16}$	0.00	0.00
17	.688	$2f_{17}^2 + 6f_{17}$	0.00	$u_{17}^2 + u_{17}$	1,453	1,453
18	1.00	$2f_{18}^2 + 800f_{18}$	$4f_{18}^2 + 80f_{18}$	$.5u_{18}^2 + 10u_{18}$	3,600	3,600
19	1.00	$f_{19}^2 + 600f_{19}$	$1f_{19}^2 + 60f_{19}$	$.5u_{19}^2 + 5u_{19}$	1,800	1,800
20	1.00	$f_{20}^2 + 300f_{20}$	$1f_{20}^2 + 30f_{20}$	$.5u_{20}^2 + 2u_{20}$	1,000	1,000

manufacturers and the end users are approximately the same (next day delivery by air or truck) and the number of end users is sufficiently large that an average transportation cost per mode can be used. A similar assumption is appropriate in the case of Canada, except as depicted in Figure 3, one generator manufacturer cannot ship to Canada via truck. While the details of transportation will vary among Mexico and the Caribbean islands, in general, this information can be represented by a single average transportation time and cost.

As can be seen from the solution in Table 1, links: 9,12,13,14 and 16, all of which are transportation links in the supply chain need not be “built” since the optimal capacities are

equal to zero and the flows, hence, are also equal to zero on these links.

Hence, the optimal supply chain network topology is as given in Figure 4. Note that we have removed all the links in Figure 3 which have zero capacities since they will not be constructed.

For completeness, we also report the optimal path flow pattern.

For  $w_1 = (0, H_1^2)$ , two paths had positive flow with the other four paths having zero flow. Specifically, the path consisting of links:(1,2,3,4,7,10,18) had its path flow equal to 4,031.45, and the path consisting of the links: (1,2,3,6,8,15,18) had a path flow of: 4,047.68.

For  $w_2 = (0, H_2^2)$ , two paths had positive flow with three others having zero flow. Specifically, the path consisting of the links (1,2,3,4,7,11,19) had a flow of 2,186.63 and the path consisting of the links: (1,2,3,5,7,11,19) had a flow of 1,880.68.

For  $w_3 = (0, H_3^2)$ , only one path had positive flow and the two others had zero flows. The path comprised of the links: (1,2,3,6,8,17,20) had a flow equal to 2,888.06.

Recall that the flows decrease as they move down the supply chain due to radioactive decay according to their respective path flow multiplier  $\mu_p$ .

The total cost associated with this supply chain network design was: 2,976,125,952.00.

The existing capacity at the Canadian reactor is 33,535, whereas the existing capacity at the processor is 32,154. Hence, one can infer from the above analysis that both of these are operating with excess capacity, which has been noted in the literature.

Of course, the above case study is stylized but it demonstrates how data can be acquired and the relevance of the output results. With the model in Section 2, a cognizant organization can then investigate the costs associated with new supply chain networks for a radioisotope used in medical imaging and diagnostics.

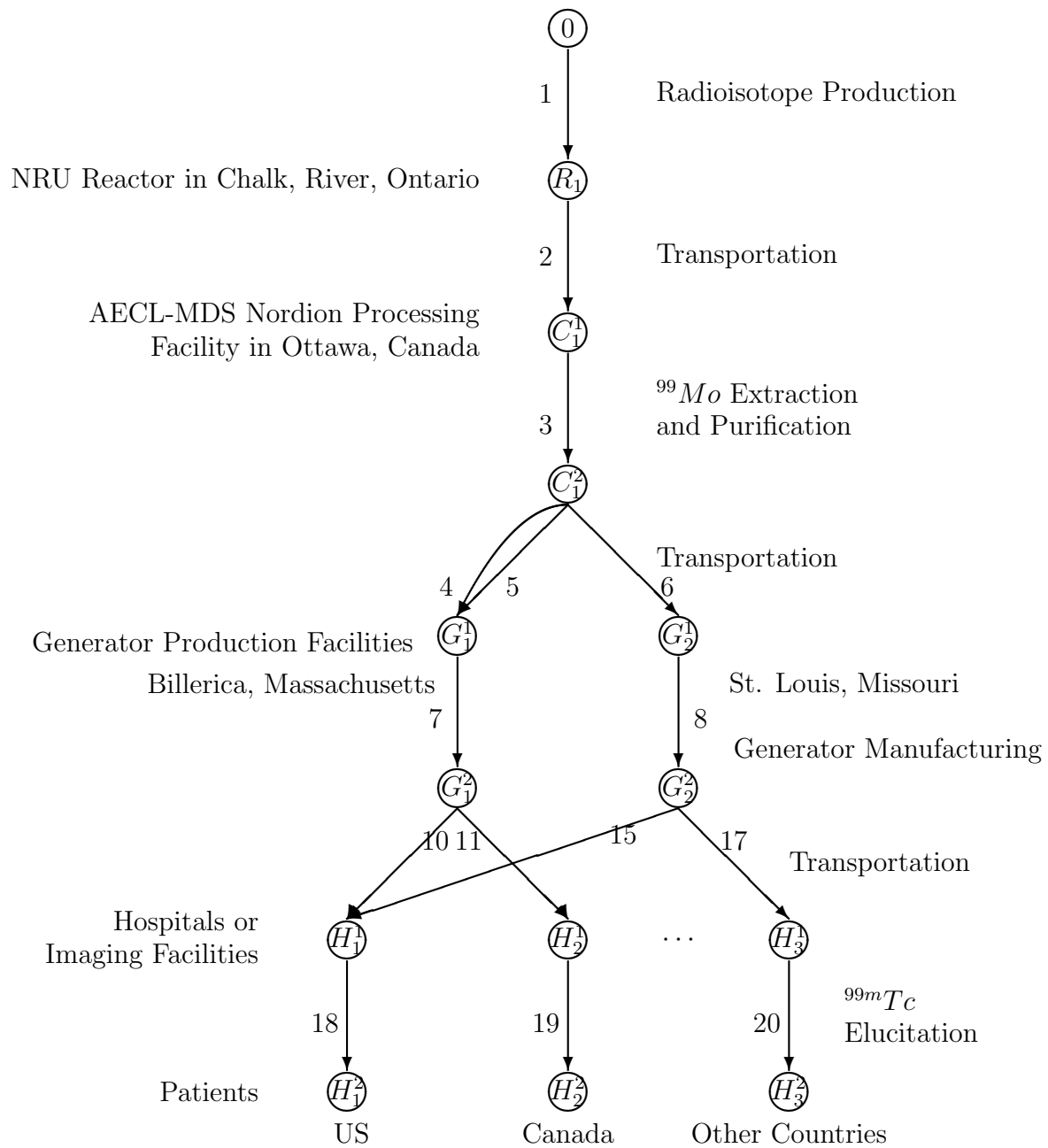


Figure 4: The Optimal Supply Chain Network for MO-99 from Canada to the United States, Canada, and Other Countries

## 5. Summary and Suggestions for Future Research

In this paper, we developed a rigorous framework for the design of medical nuclear supply chains. We focused on the most widely used radioisotope, Molybdenum,  $^{99}Mo$ , which is used in medical diagnostics for cancer and cardiac problems. Medical nuclear supply chains have numerous challenging features, including the time-sensitivity of the product, which is subject to radioactive decay, the hazardous nature of production and transportation as well as waste disposal. In addition, such radioisotopes are produced globally only in a handful of reactors and the same holds for their processing. Moreover, the nuclear reactors where they are produced are aging and have been subject to failures creating shortages of this critical healthcare product.

The specific contributions of the findings in this paper are:

- (1). a theoretically sound, based on physics principles, methodology to determine the loss, due to time-decay, of the radioisotope on the various links of the supply chain network, through the use of arc multipliers;
- (2). a generalized network optimization model that includes the relevant criteria associated with link construction, coupled with the operational costs and the associated discarding and waste management costs, subject to demand satisfaction at the patient demand points;
- (3). a unified framework that can handle the design of the medical nuclear supply chain network from scratch, with specific relevance to the existing economic and engineering situation, coupled with the physics underlying the time-decay of the radioisotope, and
- (4). an algorithm which resolves the new supply chain network design problem into sub-problems with elegant features for computation, for which we provide explicit formulae and a generalized exact equilibration algorithm to handle multipliers.

We note that the contributions in the paper can serve as the foundation for the investigation of other medical nuclear product supply chains. In addition, the framework can serve as the basis for the exploration of alternative behaviors among the various stakeholders, including competition. Finally, it can be used to assess the vulnerability of medical nuclear supply chains and to explore alternative topologies and the associated costs. Since it has

been recognized that some of such supply chains are presently operating without recovering the costs at the reactors, resulting in market failure and a lack of incentive investment, plus that the need for such medical diagnostics is expected to grow with the aging population, we believe that this paper, in emphasizing a new research agenda, has made a valuable contribution.

Further research will include additional empirical research.

### **Acknowledgments**

The first author acknowledges support from the John F. Smith Memorial Fund at the University of Massachusetts Amherst. She also acknowledges the support from the School of Business, Economics and Law at the University of Gothenburg in Gothenburg, Sweden, where she is a Visiting Professor of Operations Management for 2012-2013.

The authors appreciate the comments and suggestions on an early version of this purpose.

### **References**

- American Institute of Physics Handbook, 1972. 3rd edition, McGraw Hill, New York, NY, 8-6 - 8-91.
- Berger, S. A., Goldsmith, W., Lewis, E. R., Editors, 2004. Introduction to Bioengineering. Oxford University Press, Oxford, UK.
- Cruz, J. M., Liu, Z., 2011. Modeling and analysis of multiperiod effects of social relationship on supply chain networks. *European Journal of Operational Research*, 214, 39-52.
- de Lange, F., 2010. Covidien's role in the supply chain of Molybdenum-99 and Technetium-99m generators. *tijdschrift voor nucleaire geneeskunde*, 32,593-596.
- Kahn, L. H. The potential dangers in medical isotope production. *Bulletin of the Atomic Scientists*, March 16, 2008, <http://thebulletin.org/node/163>.
- Kochanek, K. D., Xu, J., Murphy, S. L., Minino, A. M., Kung, H.-C., 2011. Deaths: preliminary data for 2009, *National Vital Statistics Reports*, Vol. 59, No. 4, March 16.

- Lantheur Medical Imaging, Inc., 2009. Lantheur Medical Imaging takes proactive steps to mitigate impact of global molybdenum-99 supply chain operations on operations. Press Release, May 20, <http://www.lantheur.com/News-Press-2009-0520.html>.
- Liu, Z., Nagurney, A., 2011. Supply chain outsourcing under exchange rate risk and competition. *OMEGA*. 39, 539-549.
- Nagurney, A., 1999. *Network Economics: A Variational Inequality Approach*, second and revised edition. Kluwer Academic Publishers, Dordrecht, The Netherlands.
- Nagurney, A., 2006. *Supply Chain Network Economics: Dynamics of Prices, Flows, and Profits*. Edward Elgar Publishing, Cheltenham, England.
- Nagurney, A., 2010. Optimal supply chain network design and redesign at minimal total cost and with demand satisfaction. *International Journal of Production Economics*, 128, 200-208.
- Nagurney, A., Aronson, J., 1989. A general dynamic spatial price network equilibrium model with gains and losses. *Networks*, 19, 751-769.
- Nagurney, A., Masoumi, A. H., 2012. Supply chain network design of a sustainable blood banking system. In: *Sustainable Supply Chains: Models, Methods and Public Policy Implications*. T. Boone, V. Jayaraman, and R. Ganeshan, Editors, Springer, London, England, pp 49-72.
- Nagurney, A., Masoumi, A. H., Yu, M., 2012. Supply chain network operations management of a blood banking system with cost and risk minimization. *Computational Management Science*, 9(2), 205-231.
- Nagurney, A., Qiang, Q., 2009. *Fragile Networks: Identifying Vulnerabilities and Synergies in an Uncertain World*. John Wiley & Sons, Hoboken, New Jersey.
- National Research Council, 2009. *Medical isotope production without highly enriched uranium*. The National Academy of Sciences, Washington, DC.
- OECD, 2010a. *The supply of medical radioisotopes: An economic study of the molybdenum-99 supply chain*. Nuclear Energy Agency.

OECD, 2010b. The supply of medical radiosotopes: Review of potential molybdenum-99/technetium-99m production technologies. Nuclear Energy Agency.

Ponsard, B., 2010. Mo-99 supply issues: Report and lessons learned, presented at the 14th International Topical Meeting on the Research Reactor Fuel Management (RRFM 2010), Marrakech, Morocco, 21-25 March, published by the European Nuclear Society, ENS RRFM 2010 Transactions.

Qiang, Q., Nagurney, A., Dong, J.. 2009. Modeling of supply chain risk under disruptions with performance measurement and robustness analysis. In *Managing Supply Chain Risk and Vulnerability: Tools and Methods for Supply Chain Decision Makers*. Wu, T., Blackhurst, J., Editors, Springer, Berlin, Germany, pp 91-111.

Seeverens, H. J. J., 2010. The economics of the molybdenum-99/Technetium-99m supply chain. *tijdschrift voor nucleaire geneeskunde*, 32,604-608.

World Nuclear Association, 2011. Radioisotopes in medicine. January 26, <http://www.world-nuclear.org/inf55.html>.

Zhang, D., 2006. A network economic model for supply chain versus supply chain competition, *OMEGA*, 34, 283-295.